[redacted]

Copy
RM L57D25c

NACA

RESEARCH MEMORANDUM

LOCAL HEAT TRANSFER TO BLUNT NOSES

AT HIGH SUPERSONIC SPEEDS

By William E. Stoney, Jr.

Langley Aeronautical Laboratory
Langley Field, Va.

NASA ltr Dec. 6, 1962. By HYR.
dtd Nov. 14, 1962, s/ Boyd C. Myers II. Effective date: Sept. 27, 1962.

NATIONAL ADVISORY COMMITTEE
FOR AERONAUTICS

WASHINGTON

July 12, 1957

[redacted]

NATIONAL ADVISORY COMMITTEE FOR AERONAUTICS

RESEARCH MEMORANDUM

LOCAL HEAT TRANSFER TO BLUNT NOSES AT HIGH SUPERSONIC SPEEDS

By William E. Stoney, Jr.

SUMMARY

A brief summary is presented of the recent theoretical and experimental work on local heat-transfer rates on blunt-nose bodies. Comparisons of theoretical and measured heating rates indicate the following conclusions: The calculation of local conditions over noses of high radius of curvature needs more study and testing at the present time. If local flow conditions are known, the laminar heating rates over the whole nose shape can be calculated within most engineering accuracy requirements for the whole range of Mach numbers up to 13.8. For the case of turbulent flow, turbulent flat-plate theory based on local flow properties can provide good estimates of the heating rates possible. The prediction of transition remains at present the biggest unknown.

INTRODUCTION

The importance of blunt-nose shapes has increased in recent years because such shapes have many advantages in comparison with the more common sharp-nose shapes for missiles having high heating rates. High drag is sometimes desirable for ballistic missiles and does not penalize the total efficiency of these missiles since they operate at essentially drag-free altitudes for the major part of their flight. As shown in reference 1, extremely blunt noses develop lower total heating rates than do sharp noses of about the same size and weight. Finally, and perhaps most importantly, there are many indications that extremely blunt shapes foster longer runs of laminar flow than do sharp shapes.

For these reasons the calculation of the local heating rates on such shapes has become extremely important. The present paper gives a brief summary of present-day techniques and their effectiveness. This summary together with the attached list of references should be helpful to those orienting themselves in this fast-changing field.

SYMBOLS

C_p	pressure coefficient
l	surface distance measured from stagnation point
M	Mach number
p	pressure
q	heating rate, Btu/(sec)(sq ft)
$R_{\infty,d}$	free-stream Reynolds number based on body diameter
r_b	base radius
r_h	nose radius or radius of curvature
s	surface distance from stagnation point to junction of hemisphere and cylinder; on flat face, distance from stagnation point to edge, that is, cylinder radius
T	temperature, $^{\circ}$F
x	distance along center line measured from apex of nose
θ	angle between free stream and normal to surface of nose
μ	viscosity of air
ρ	density of air

Subscripts:

HEMIS	hemispherical nose
l	local
w	based on temperature of wall surface
0	at stagnation point
∞	free stream

[redacted]

Calculation of Local Flow Conditions

Before any attempt can be made to calculate heat-transfer rates, the local flow conditions must be calculated. Blunt noses can be classified roughly into two groups: those for which the Newtonian flow concept $\left(C_{p,l}/C_{p,0} = \cos^2\theta\right)$ is applicable and thus for which the local conditions can be easily calculated, and those for which the Newtonian flow concept is not applicable and for which no simple solutions exist.

A rough boundary can be fixed between these two groups of nose shapes by consideration of a series of noses having constant radii of curvature. Such a series is illustrated in figure 1; this series progresses from the hemispherical nose on the left to the flat nose (infinite radius) on the right. The intermediate case for this series would be the nose shown in the center - the nose for which, according to Newtonian theory, the flow just before the corner is at a Mach number of 1. Until stricter criteria are provided, Newtonian calculations should be checked with experiment or with a more comprehensive theory for noses having a radius of curvature at the stagnation point greater than $\sqrt{2}r_b$. Recently, several theoretical approaches have been presented to the blunt-nose problem. (See refs. 2 to 5; theories presented in refs. 4 and 5 may also be found in appendix D of ref. 6.) Some of these appear to be promising, but more experience with them is needed before their general usefulness can be determined.

This paper considers only shapes whose local conditions are known. Experimental data and theoretical results are applied to the hemispherical and the flat noses to bring out the following points:

(1) If the rate of change of velocity at the stagnation point is known, the heat-transfer rate at this point can be calculated accurately enough for most engineering purposes.

(2) With the proper pressure distribution the laminar heating rates over the entire nose can be calculated satisfactorily, and reasonably good estimates of the possible turbulent heating rates can be made.

Prediction of Stagnation-Point Heating Rates

The prediction of stagnation-point heating rates is well proved for the lower Mach number range and needs demonstration only at the higher Mach numbers where real gas effects come into play.

In figure 2 the ratios of measured stagnation-point heating rates to theoretical calculations are presented as functions of free-stream Mach number. The test results were obtained from a flight of the Lockheed X-17 rocket having a nose defined by the equation $r/r_b = (x/2r_b)^{1/3}$ (ref. 6), a flat-face NACA rocket model, and AVCO shock-tube experiments (ref. 7). The curves for the rocket data represent the Mach number time history for the flight, the lower portion being that for the accelerating part of the flight and the upper portion representing the decelerating Mach numbers. The difference between accelerating and decelerating values at any given Mach number is probably a measure of the test accuracy rather than a real effect due to the higher Reynolds numbers of the deceleration portion of the flight path.

The theoretical heating rates were calculated by the stagnation-point theory of Fay and Riddell (ref. 8) for the equilibrium boundary layer with a Prandtl number of 0.71 and a Lewis number of 1.4. The general conclusion to be derived from this figure is that, although the scatter shown indicates that many details of the heat-transfer processes under these high-temperature conditions are still unknown, the agreement of these data is close enough so that it can be felt that their general nature is understood.

Calculation of Heating Rates Over Entire Nose

In the calculation of heating rates over the entire nose, the stagnation-point heat-transfer rates of the hemispherical noses are used as datum points, and all the data and calculations are presented as ratios of these values.

Figure 3 presents the ratios of local laminar heating rates on a hemispherical nose to stagnation heating rates plotted as functions of position along the surface of the hemisphere. The test points are for a variety of conditions from $M_\infty = 2$ to 6.8 and free-stream Reynolds numbers based on diameter of 1.0×10^6 to 14.3×10^6. (Data for $M = 2$ and $M = 3.9$ are presented in ref. 9; data for $M = 6.8$ in ref. 10; and data for $M = 2.5$ in ref. 11.) Good agreement with the theoretical distributions, which were calculated by the method of Lees (ref. 12), can be seen immediately. It is important to notice that the distribution of heating rates does not vary markedly with Mach number.

Another interesting condition indicated by the data in figure 3 is the extremely high Reynolds number $\left(14.3 \times 10^6\right)$ for which laminar flow was obtained in one flight test. This model, however, was a special case for which extreme pains were taken to obtain a mirror finish on the nose of the order of 2 microinches - not an ideal process for assembly-line fabrication.

Similar agreement with test results can be shown for the other extreme in the series of nose shapes - the perfectly flat face. In figure 4 the local heating rates were not divided by the flat-face stagnation heating rates but by the appropriate hemispherical stagnation heating rates. This allows a direct comparison of the flat and hemispherical values. The solid line gives the theoretical laminar results for the flat face by the method of Lees (ref. 12); and the dashed line above it, the same ratio calculated by the method of Stine and Wanlass (ref. 13). The latter calculations differ from Lees' because they include a correction for the effect of pressure gradient. (For the relatively low pressure gradients of the hemisphere, the two methods agree closely.) As can be seen from the figure the agreement with either theory is reasonably good and the uncertainties in the measurements do not permit a choice between them.

Since the flat nose is a shape for which Newtonian flow concepts do not work at all, a pressure-ratio distribution p_l/p_0 obtained experimentally at a Mach number of 2 (see also theoretical distribution of ref. 14) was assumed to be constant for all higher Mach numbers and was used in the theoretical calculations. The agreement of the data, which cover Mach numbers from 2 to 13.8, indicates that this approximation was adequate for this case. (Data were obtained for $M = 2$ in the preflight jet and for $M = 13.8$ in free flight at the Langley Pilotless Aircraft Research Station at Wallops, Island, Va., and data for $M = 5$ were determined in an investigation of 2-inch flat-face cylinders conducted by Morton Cooper in the Mach number 5 axisymmetric blowdown jet at the Langley Gas Dynamics Branch.)

What is gained by the flat face in lower local heating rates in the center is lost at its edge. However, it must be remembered that high local heating rates are not necessarily the critical points in a particular design, as can be shown by the time history of temperature profiles on the front and side of the flat-face rocket model on which the heating rates at a Mach number of 13.8 were obtained. These temperature profiles and a sketch of the nose are presented in figure 5. The nose was made of copper and was three-sixteenths of an inch thick on the front and one-eighth of an inch thick at the sides. The datum points represent the temperatures as measured along the front surface and down the side for three different times during the high Mach number part of the flight. At the earliest time not much heating has occurred and the temperature profile is relatively flat. At peak Mach number the effects of conduction in the skin can be seen since the highest temperature is reached at $0.8l/s$ in spite of the peak heating which occurs at the corner. The reason that the sides are able to act as good heat sinks lies in their extremely low heating rates. Measurements of these rates for the first two side thermocouples are shown in figure 4. Seven seconds later, the model has slowed down to a Mach number of 7, and the lateral flow of heat in the skin was so large that the maximum temperature of the flight occurred in the center of the model - not at the corners. This is, of course, only an example but it does show that a fairly detailed study of the particular nose must be made if its effectiveness is to be evaluated correctly.

There are some indications (for example, ref. 1) that flat noses or closely allied shapes may have some advantages in retaining laminar flow, and, as is shown, on a hemispherical nose this retention can be very important since turbulent heating rates can be very high. In figure 6 the ratios of local heating rates to stagnation heating rates are presented as functions of surface location. The test points were determined from an investigation conducted by Ivan E. Beckwith and James J. Gallagher in a blowdown jet at the Langley Gas Dynamics Branch. For this investigation a Mach number of 2 and free-stream Reynolds numbers (based on body diameter) of 2.7×10^6 and 3.4×10^6 were used. Transition obviously took place forward on the hemisphere for both tests and heating rates nearly $2\frac{1}{2}$ times the stagnation rate were reached. The solid line represents flat-plate turbulent values based on the local Reynolds numbers around the body. This comparison and similar comparisons from other tests indicates that even this relatively crude theoretical approach may have considerable value in estimating the turbulent heating rates. (See also ref. 15 and appendix C of ref. 6.)

CONCLUDING REMARKS

The calculation of the local flow conditions over noses of high radius of curvature needs more investigation at the present time, although data obtained in low Mach number tests may be adequate at much higher Mach numbers for use in these calculations. However, if the local conditions are known, the laminar heating rates over the whole nose shape can be calculated within most engineering accuracy requirements for the whole range of Mach numbers up to at least 13.8.

For turbulent flow, flat-plate theory may provide good estimates of the heating rates possible. Of course, the prediction of transition still remains and is the biggest unknown at the present time.

Langley Aeronautical Laboratory,
National Advisory Committee for Aeronautics,
Langley Field, Va., March 6, 1957.

REFERENCES

1. Allen, H. Julian, and Eggers, A. J., Jr.: A Study of the Motion and Aerodynamic Heating of Missiles Entering the Earth's Atmosphere at High Supersonic Speeds. NACA RM A53D28, 1953.

2. Maslen, Stephen H., and Moeckel, W. E.: Inviscid Hypersonic Flow Past Blunt Bodies. Preprint No. 665, S.M.F. Fund Preprint, Inst. Aero. Sci., Jan. 1957.

3. Probstein, Ronald F.: Inviscid Flow in the Stagnation Point Region of Very Blunt-Nosed Bodies at Hypersonic Flight Speeds. WADC TN 56-395 (Contract No. AF 33(616)-2798), Wright Air Dev. Center, U. S. Air Force, Sept. 1956. (Also available from ASTIA as Doc. No. AD97273.)

4. Hayes, Wallace D.: Some Aspects of Hypersonic Flow. The Ramo-Wooldridge Corp., Jan. 4, 1955.

5. Hayes, Wallace D.: Hypersonic Flow Fields at Small Density Ratio. Doc. No. 34, The Ramo-Wooldridge Corp., May 12, 1955.

6. Anon.: X-17 Re-Entry Test Vehicle - R-3 Final Flight Report. Rep. No. MSD-3013 (Contract No. AF 04 (645)-7), Lockheed Aircraft Corp., Oct. 31, 1956.

7. Rose, P. H., and Stark, W. I.: Stagnation Point Heat Transfer Measurements in Air at High Temperature. Res. Note 24, AVCO Res. Lab., Dec. 11, 1956.

8. Fay, J. A., and Riddell, F. R.: Stagnation Point Heat Transfer in Dissociated Air. Res. Note 18, AVCO Res. Lab., June 1956.

9. Garland, Benjamine J., and Chauvin, Leo T.: Measurements of Heat Transfer and Boundary-Layer Transition on an 8-Inch-Diameter Hemisphere Cylinder in Free Flight for a Mach Number Range of 2.0 to 3.88. NACA RM L57D04a, 1957.

10. Crawford, Davis H., and McCauley, William D.: Investigation of the Laminar Aerodynamic Heat-Transfer Characteristics of a Hemisphere-Cylinder in the Langley 11-Inch Hypersonic Tunnel at a Mach Number of 6.8. NACA TN 3706, 1956.

11. Buglia, James J.: Heat Transfer and Boundary-Layer Transition on a Highly Polished Hemisphere-Cone in Free Flight at Mach Numbers Up to 3.14 and Reynolds Numbers Up to 24×10^6. NACA RM L57D05, 1957.

12. Lees, Lester: Laminar Heat Transfer Over Blunt-Nosed Bodies at Hypersonic Flight Speeds. Jet Propulsion, vol. 26, no. 4, Apr. 1956, pp. 259-269.

13. Stine, Howard A., and Wanlass, Kent: Theoretical and Experimental Investigation of Aerodynamic-Heating and Isothermal Heat Transfer Parameters on a Hemispherical Nose With Laminar Boundary Layer at Supersonic Mach Numbers. NACA TN 3344, 1954.

14. Maccoll, J. W., and Codd, J.: Theoretical Investigations of the Flow Around Various Bodies in the Sonic Region of Velocities. British Theoretical Res. Rep. No. 17/45, B.A.R.C. 45/19, Ministry of Supply, Armament Res. Dept., 1945.

15. Van Driest, E. R.: The Problem of Aerodynamic Heating. Aero. Eng. Ref., vol. 15, no. 10, Oct. 1956, pp. 26-41.

BLUNT-NOSE FLOW FIELDS

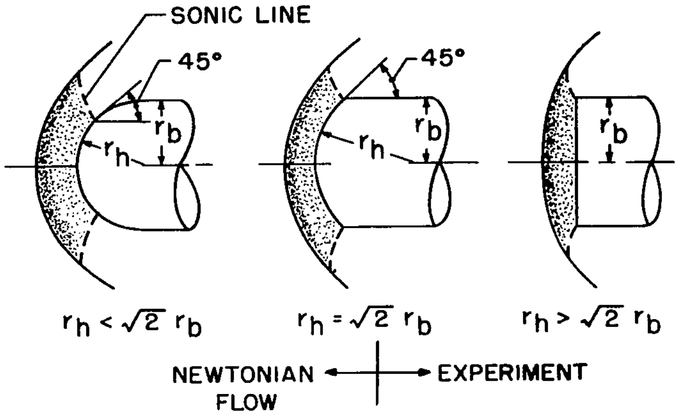

Figure 1

COMPARISON OF MEASURED AND CALCULATED STAGNATION HEAT-TRANSFER RATES

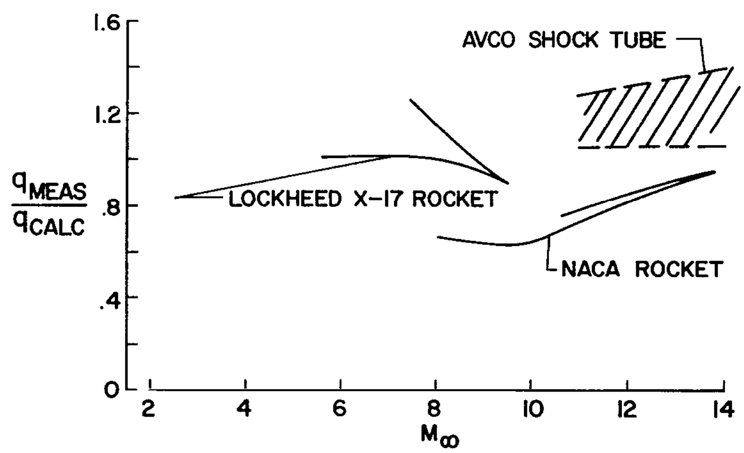

Figure 2

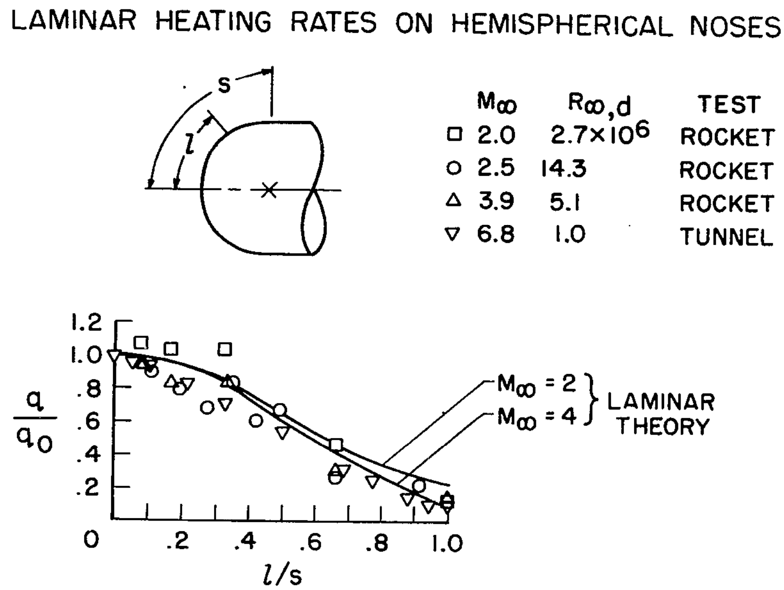

Figure 3

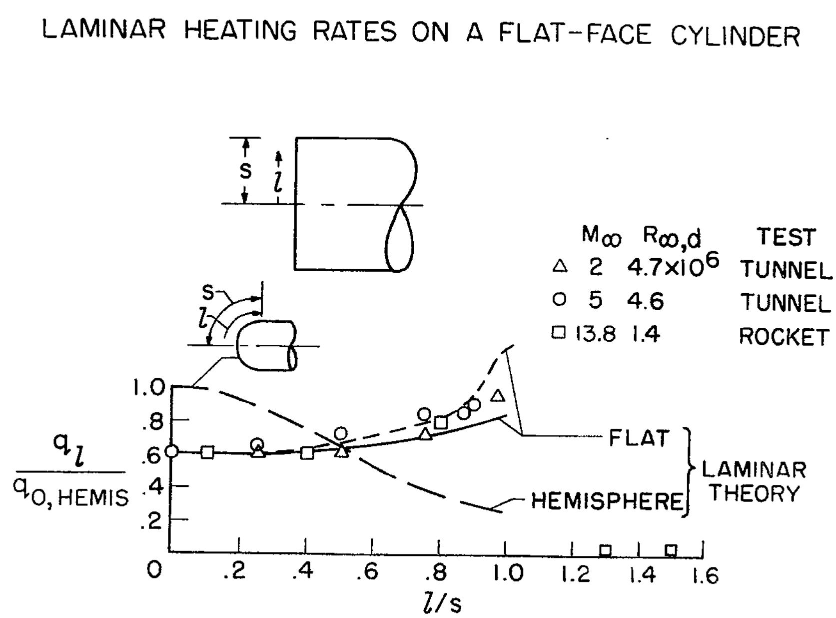

Figure 4

TEMPERATURE HISTORY ON FACE AND SIDES OF ROCKET MODEL

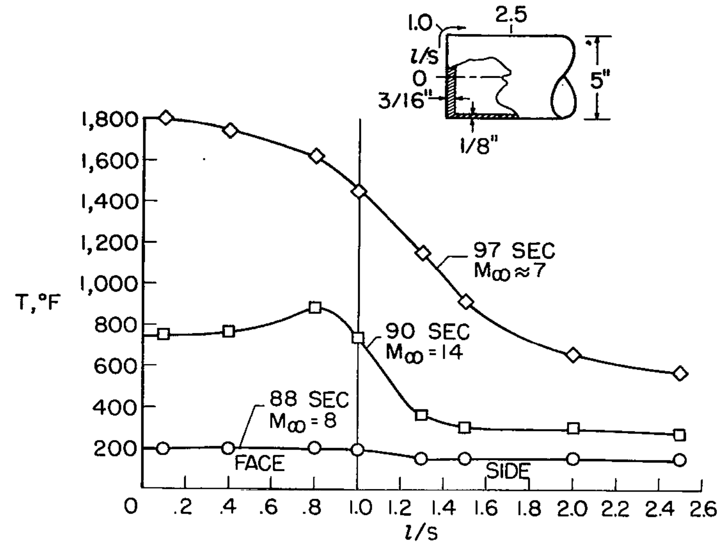

Figure 5

TURBULENT HEATING RATES ON A HEMISPHERICAL NOSE

TUNNEL TESTS AT $M_\infty = 2$

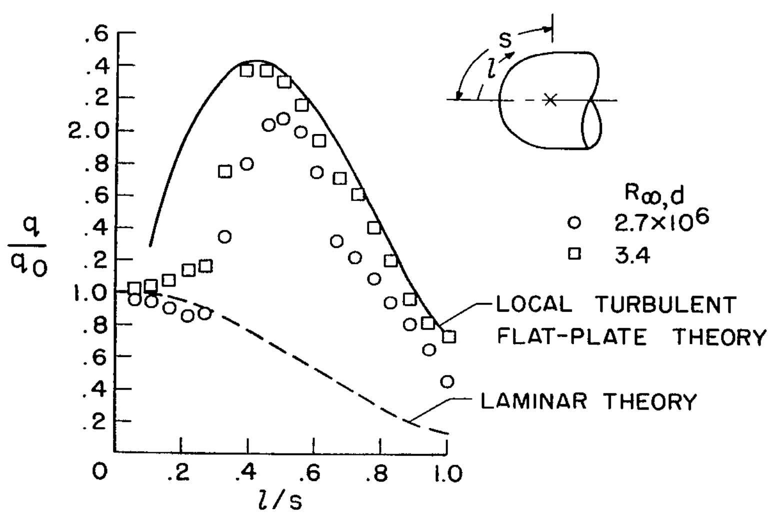

Figure 6

NACA - Langley Field, Va.